



Research Report

How the brain encodes morphological constraints during Chinese word reading: An EEG-fNIRS study



Fei Gao^{a,b}, Ruien Wang^{a,c}, Paulo Armada-da-Silva^{a,d}, Meng-Yun Wang^e, Hai Lu^f, Chantat Leong^{a,d} and Zhen Yuan^{a,d,*}

^a Centre for Cognitive and Brain Sciences, University of Macau, Macau SAR, China

^b Faculty of Arts and Humanities, University of Macau, Macau SAR, China

^c Faculty of Social Sciences, University of Macau, Macau SAR, China

^d Faculty of Health Sciences, University of Macau, Macau SAR, China

^e Faculty of Psychology, University of Bergen, Bergen, Norway

^f Spinal Surgery, Fifth Affiliated Hospital of Sun Yat-sen University, Zhuhai, China

ARTICLE INFO

Article history:

Received 30 March 2021

Reviewed 22 June 2021

Revised 13 July 2021

Accepted 25 May 2022

Action editor Jean-Francois

Demonet

Published online 13 June 2022

Keywords:

Morphological constraints

Complex word

Chinese reading

Fused EEG-fNIRS

ABSTRACT

Although the role of morphology in alphabetic language processing has been extensively studied, it is still unclear how morphology is enabled and constrained in morpho-syllabic languages like Chinese. This study aims to inspect the time courses and patterns of brain activation associated with Chinese morphological constraint encoding. Chinese native speakers were recruited to perform visual lexical decisions on real Chinese compound words, pseudowords, and nonwords, whilst behavioral, electroencephalographic, and functional near infrared spectroscopy data were simultaneously recorded. For the first time, both morphological and semantic effects were examined to reveal the corresponding spatio-temporal brain activation patterns based on multimodal data. Brain activation differences between pseudowords and real words indexed morphological sensitivity, whereas differences between real words or pseudowords and nonwords characterized semantic effects. Electrophysiological data showed that semantic processing occurred earlier (N400, 300–450 msec) than morphological processing (450–570 msec), while brain activation patterns revealed a differentiation between morphological parsing (specified in the left inferior frontal gyrus) and semantic analysis (in a broader fronto-temporal network). These findings offer new evidence that morphological constraints are encoded at a late stage of compound word processing in Chinese and suggest that the left prefrontal cortex plays an essential role in this process.

© 2022 Elsevier Ltd. All rights reserved.

* Corresponding author. Centre for Cognitive and Brain Sciences, University of Macau, Macau SAR, China.

E-mail address: zhenyuan@um.edu.mo (Z. Yuan).

<https://doi.org/10.1016/j.cortex.2022.05.016>

0010-9452/© 2022 Elsevier Ltd. All rights reserved.

1. Introduction

To reveal how words are encoded and constrained by the human brain, it is essential to identify the complex neuro-cognitive mechanism underlying morpho-semantic processing. Morphological processing involves mental operations on internal morphemic information and structure of a given word, and this whole process is always intertwined with semantic analysis (Chung, Tong, Liu, McBride-Chang, & Meng, 2010; Ip et al., 2017). To date, although the role of morphology in alphabetic language processing has been extensively explored (e.g., Bölte, Jansma, Zilverstand, & Zwitserlood, 2009; Carrasco-Ortiz and Frenck-Mestre, 2014; Leminen, Smolka, Dunabeitia, & Pliatsikas, 2019; Schremm, Novén, Horne, & Roll, 2019), it is yet unclear how Chinese morphology is represented during reading process. As more than 70% of Chinese words are formed by compounding two or three constitute characters/morphemes, written Chinese is often described as morpho-syllabic (DeFrancis, 1989), where each character corresponds to a single syllable/morpheme. Therefore, constitute morphemes at the sub-lexical level might play an important role in mediating lexical access and processing of the whole words. Recently, a growing body of studies have demonstrated the psychological reality of morpheme effect and sub-lexical processing in Chinese compound word reading (e.g., Huang, Lee, Huang, & Chou, 2011; Huang, Lee, Tsai, & Tzeng, 2011; Zhao, Wu, Li, & Guo, 2017; Gao, Wang, Zhao, & Yuan, 2021). However, it is still poorly understood how the human brain encodes the spatio-temporal signature of morphological constraints during Chinese word reading.

Interestingly, the time course and temporal signature of Chinese morphological structure processing have been inspected by using coordinative compounds (e.g., “花草”/faa1 cou2/, flower–grass, plant) embedded in a visual priming lexical decision task (Chung et al., 2010). Event-related potential (ERP) results showed that the pure morphological structure effect was only detected in the time window of 220–300 msec (the frontal P250/P2 effect), while the classic N400 semantic priming effect (manifested at centro-parietal electrode sites) was able to index the semantic memory network activation, indicating that morphological structure might automatically modulate the semantic processing during early-stage compound word reading (Pylkkänen & Marantz, 2003; Pylkkänen, Feintuch, Hopkins, & Marantz, 2004). An additional study also illustrated that word pairs with identical morphological structure elicited greater P2a amplitudes (150–180 msec at the frontal sites) than those with distinct structures (Gu, Yu, & Ma, 2012). These findings suggested that there might exist a morphological structure processing component at the early stage of Chinese compound word reading, which is independent of the later-stage lexico-semantic processing. Contrary to the early processing account (e.g., P250/P2, P2a), nevertheless, a bunch of recent investigations demonstrated that Chinese morphological processing implicates a conscious process at the post-lexical level (Allen, Badecker, & Osterhout, 2003; Newman, Ullman, Pancheva, Waligura, & Neville, 2007). For example, it was discovered that words of higher morphological productivity (i.e., subordinate structure) elicited significantly larger P600

amplitudes at the frontal sites of the scalp than those of lower morphological productivity (i.e., coordinate structure), whereas no early P150 or semantic N400 was detected to be associated with distinct morphological structures (Gu and Yang, 2010). In particular, the P600 effect was interpreted as an index of late re-analysis on structural productivity or morphological structure information, which might involve a conscious processing on Chinese compound word recognition. However, the discrepancy between the early and late processing accounts on Chinese morphological information could be attributed to differing task natures (e.g., with or without priming) and distinctive word structures under investigation across studies. It is therefore essential to better understand the temporal signature of Chinese morphological structure processing with more fine-grained designs.

Besides, decoding spatial neural activation patterns associated with Chinese morphological structure processing is also extremely important to explore the neural bases of Chinese morphology. Previous studies have revealed that lexical access and morphological awareness involve the semantic brain networks such as the ventral inferior frontal gyrus [IFG, Brodmann's Area (BA) 45/47] and the left middle temporal gyrus (MTG, BA 21/37) (Arredondo, Ip, Shih Ju Hsu, Tardif, & Kovelman, 2015; Bick, Frost, & Goelman, 2010; Booth et al., 2006; Chee, O'Craven, Bergida, Rosen, & Savoy, 1999; Hsu, Pylkkänen, & Lee, 2019; Liu et al., 2009, 2013), which are sensitive to the salient morpho-syllabic feature of Chinese language. In particular, it was discovered that morphological structure task elicited robust activations in the dorsal IFG and the posterior superior temporal gyrus (STG), as well as the ventral IFG and the posterior MTG, indicating that Chinese morphological processing engages both the left frontal and temporal regions (Liu et al., 2013; Arredondo et al., 2015; Zou, Packard, Xia, Liu, & Shu, 2016; Ip et al., 2019). However, the abovementioned findings were either dependent on auditory input (e.g., Ip et al., 2019; Zou et al., 2016), or among children (e.g., Arredondo et al., 2015; Liu et al., 2013). It is yet unclear whether the identified neural activation patterns might remain in visual modality for adult Chinese readers.

The current study is therefore concerned with the spatio-temporal brain activation patterns associated with morphological constraint encoding during Chinese compound word reading. We operationalized morphological constraint as the sensitivity to morphological structure legality and structural difficulties in reading words. Specifically, we created semantically interpretable pseudowords to probe this sensitivity and indicate morphological constraints (Bölte et al., 2009), as these pseudowords could reflect the structural problems when language users were mapping the plausible forms to existing lexical entries in their mental lexicon. Along with interpretable pseudowords, our study included Chinese disyllabic compound words and uninterpretable nonwords (false words) to work as baselines for evaluating distinctive mental processes. The comparison between the real words versus pseudowords indexes morphological sensitivity, while the contrast between the real/pseudowords and nonwords might reflect the process of semantic analysis. In particular, Bölte et al. (2009) detected an ERP difference between interpretable/uninterpretable pseudowords and existing German adjectives in sentential context in the left frontal electrode sites from 450 to 500 msec

after word onset, while there was no statistical difference in the semantic N400 or N400-like time window (350–450 msec) (Janssen, U., Wiese, & Schlesewsky, 2006; Leinonen, Brattico, Järvenpää, & Krause, 2008). The authors interpreted the data as a left anterior negativity (LAN) effect, which was associated with (morpho)syntactic errors (Morris & Holcomb, 2005; Rossi, Gugler, Friederici, & Hahne, 2006) in existing studies and also a structural problem due to morphological parsing in their study. As such, N400 and LAN would serve as the potential indicators of semantic and structural processing in the current study, in addition to early components like the structural P250/P2 or P2a (Chung et al., 2010; Gu et al., 2012).

Instead of manipulating morphological structures in a structural priming paradigm (e.g., Chung et al., 2010; Gu et al., 2012), however, the current study included five sub-structures of Chinese compounding, based on their distributional proportions in natural language, in an attempt to depict the general morphological constraints as a linguistic module (parallel to semantics). Meanwhile, as different word structures were used in our study where structural priming might introduce potential confounding factors, we focused on the isolated words in a lexical decision task (Gu et al., 2010) instead of employing a priming paradigm. In addition, electroencephalography (EEG) and functional near-infrared spectroscopy (fNIRS) were recorded simultaneously to depict *when*, *where*, and *how* Chinese morphological processing is encoded in the human brain during compound word reading. EEG is informative about the neural processing of a given stimulus on millisecond-by-millisecond basis (Luck, 2014), whereas fNIRS can localize changes of the hemodynamic responses in the human cerebral cortex. The combination of these two technologies can provide new and valuable information on neurovascular coupling mechanism, thus paving a new avenue for precisely and comprehensively examining the spatio-temporal neural activity associated with morphological constraints during Chinese words reading.

Our predictions were as follows. First, we expected that pseudowords would generate the longest reaction time and the lowest accuracy rate relative to baseline conditions, as pseudowords manifested both morphological constraints (as compared to real words) and semantic characteristics (as compared to nonwords). Then, ERP results would provide further evidence on the temporal signatures of morphological and semantic processing. If morphological sensitivity precedes semantic analysis in the time course of Chinese compound word reading, there would be a difference in the P2a component between pseudowords and real words prior to the semantic N400. Otherwise, we expected that the difference would appear at a later time window (e.g., LAN), which would index a controlled process at the post-lexical level for morphological constraint encoding. In either case above, we predicted a semantic N400 effect between real/pseudowords and nonwords, which is independent of morphological parsing in terms of temporal signatures. In contrast, if morphological constraint encoding did not hold an independent representation in the mental lexicon, the biphasic pattern of P2a-N400 or N400-LAN would not be observed. As for brain localizations, we expected the activation difference between pseudowords and real words in the left frontal and/or temporal cortex, which would be consistent with the patterns in auditory and children

studies. Importantly, it would be interesting to observe a disassociation between morphological and semantic processing in the human brain in light the fNIRS data.

2. Materials and methods

2.1. Participants

We report how we determined our sample size, all data exclusions, all inclusion/exclusion criteria, whether inclusion/exclusion criteria were established prior to data analysis, all manipulations, and all measures in the study.

Thirty Chinese-Mandarin native speakers (18 females) were recruited from the University of Macau campus. Sample size of the present study was in line with previous studies which measured the similar ERP components and hemodynamic responses in Chinese word reading process (Pan & Jared, 2020; Wu, Chang, Qiu, & Joseph, 2020; Zhang, Zhang, Peng, & Bai, 2016). All participants aged from 19 to 31 years old (mean age: 24.9) were right-handed as assessed by Edinburgh Handedness Inventory (Oldfield, 1971), with normal or corrected-to-normal vision. None of the participants reported a history of neurological or psychiatric disorders. The above-mentioned inclusion and exclusion criteria were established before the data collection. Prior to the experiment, participants signed consent forms. All the procedures were approved by the Ethics Committee of the University of Macau. No part of the study procedures and analyses was pre-registered prior to the research being conducted.

2.2. Task and stimuli materials

The task consisted of three categories of stimuli including Chinese real words, pseudowords, and nonwords. In particular, 45 high-frequency (occurrence >50 per million) Chinese disyllabic compound words served as real word materials, which were selected from CNCORPUS dataset (Jin et al., 2005, dataset size: 20 million, www.cncorpus.org/). In addition, pseudowords were created by replacing a character morpheme of a compound word from the dataset with a semantically related morpheme (e.g., synonyms, antonym) (Bölte et al., 2009; Ip et al., 2019), which need to satisfy the structural constraint of morphological compounding in Chinese (i.e., coordinate, subordinate, verb–resultative, subject–predicate, and verb–object, Huang & Liao, 2011; Liao, 2014). For example, the pseudoword “微笑” (“微”/wei1/means “mild” and “哭”/ku1/means “crying”, yet “微笑” does not exist in Chinese dictionary) was derived from the real word “微笑” (“微”/wei1/means “mild” and “笑”/xiao4/means “smile” or “laugh”, and “微笑” means “smile”, which is a real word in Chinese dictionary). From the real word “微笑” to the pseudoword “微笑”, morphological structure remained unchanged (i.e., subordinate). By contrast, nonwords were generated by combining any two characters from the mentioned dataset, which turned out a pronounceable, meaningless, and morphologically illegal string (Leong, Cheng, & Tan, 2005), such as “负各” (/fu4 ge4/, literal meaning: minus+every, it does not make any sense).

Importantly, 20 professional raters with Chinese linguistics background were invited to assess the reliability of structural

Table 1 – The structural constraints of real words and pseudowords for the present work.

Morphological structures	Pseudowords		Real words		Real words in dictionary
	Example ²	Percentage	Example ³	Percentage	Percentage
Subordinate	冷情/leng3 qing2/	60%	黑板/hei1 ban3/	47%	54%
Coordinate	街路/jie1 lu4/	18%	城市/cheng2 shi4/	38%	26%
Verb-object	离学/li2 xue2/	20%	扫地/sao3 di4/	9%	18%
Verb-resultative	获到/huo4 dao4/	2%	说明/shuo1 ming2/	4%	2%
Subject-predicate	/	0%	晚安/wan3 an1/	2%	1%

constraint of pseudoword strings with the following criteria: “Do you think it is morphologically legal? If so, please specify the morphological structure from the five abovementioned options.” According to the survey results, averaged consistency on morphological structure specification was 90.44% [95% Confidence Interval (CI): 88.4%–92.4%] across all pseudowords. In light of previous studies creating semantically interpretable pseudowords (Longtin & Meunier, 2005; Meunier & Longtin, 2007; Tseng, Lindsay, & Davis, 2020), 76 Chinese native speakers were then asked to make a Yes/No response to decide whether the given character strings (pseudowords and nonwords) were semantically interpretable. More than 50% of the raters evaluated the given pseudowords as ones with transparent definitions (Mean = 74%, SD = 14%), as opposed to ratings to nonwords (Mean = 8%, SD = 7%), which was consistent with previous criteria (e.g., Meunier & Longtin, 2007). Further, 59 raters were invited to rate the semantic plausibility of real words, pseudowords, and nonwords on a Likert scale, in which 0 denotes “not plausible” while 6 denotes “very plausible”. Pseudowords were judged as interpretable (3 and above) by more than half raters. Averaged semantic plausibility ratings for real words, pseudowords, and nonwords were 6 (95% CI: 6 to 6), 3.40 (95% CI: 3.2 to 3.6), and .54 (95% CI: .447 to .634), respectively.

Altogether, 45 pseudowords were determined for experimental stimuli. The occurrences of subordinate, coordinate, verb-object, verb-resultative, and subject-predicate structures in pseudoword and real-word group were 27, 8, 9, 1, 0, and 21, 17, 4, 2, 1, respectively, which were comparable to their distribution in Chinese dictionary (statistics from Su, 2016, see Table 1).¹

Further, three individual groups of 45 pseudowords, 45 nonwords, and 15 real-word fillers were effectively evaluated by 22 Chinese linguistics experts with a Yes/No criteria: “Do you think it is morphologically legal or not?” It was observed that the “yes” response to pseudowords was significantly higher than that from nonwords, $t(44) = 35.687, p < .001, d = 5.32$ (Table 2). Besides, multiple comparisons between the three conditions were also performed in terms of position frequency statistics (head and end). The statistics of lexical properties in Table 2 demonstrated that the position frequency (both head and end) of nonwords was significantly lower than those from

¹ A Kruskal–Wallis H test showed that there was no significant difference in word structure percentage across three sources, $\chi^2(2) = .066, p = .973$, with a mean rank structure percentage of 7.70 for pseudowords, 8.40 for real words, and 7.90 for dictionary distribution.

² Literal meaning of “冷情”: cold+feeling; “街路”: street+road; “离学”: leave+school; “获到”: gain+to.

³ Word meaning of “黑板”: blackboard; “城市”: city; “扫地”: sweep the floor; “说明”: explain; “晚安”: good night.

the real words and pseudowords ($ps < .05$), while no significant difference was identified between the real words and pseudowords ($ps > .05$)⁴. Meanwhile, no significant difference between the three conditions was identified with respect to stroke numbers and constitute character frequency ($ps > .1$).

2.3. Paradigm and procedures

Participants were seated in a comfortable chair in a dimly lit room, with approximately 80 cm from the computer monitor (Fig. 2A). Before the formal test, there was a practice session with 3 real-word and 3 non-word trials. Participants were instructed to determine whether the character string on the probe screen was a real Chinese word or not by pressing the corresponding buttons labeled on the keyboard. After the practice, participants were asked to rest for 30 sec and then proceed to perform the tasks with three blocks.

Each of the three blocks contained 15 trials for real words, 15 for pseudowords, 15 for nonwords, and 5 trials for real-word fillers. The order of all stimuli within each block was randomized. There was a 1-min interval between two consecutive blocks to allow the participants to have a break. Each trial (Fig. 1) started with a fixation cross (500 msec) displaying at the center of the monitor, followed by the presentation of a blank (200 msec), the stimulus onset (400 msec), the probe of two question marks (≤ 3000 msec), and a red cross indicating a rest (12000 msec), respectively. It took about 40–50 min to finish the whole experiment.

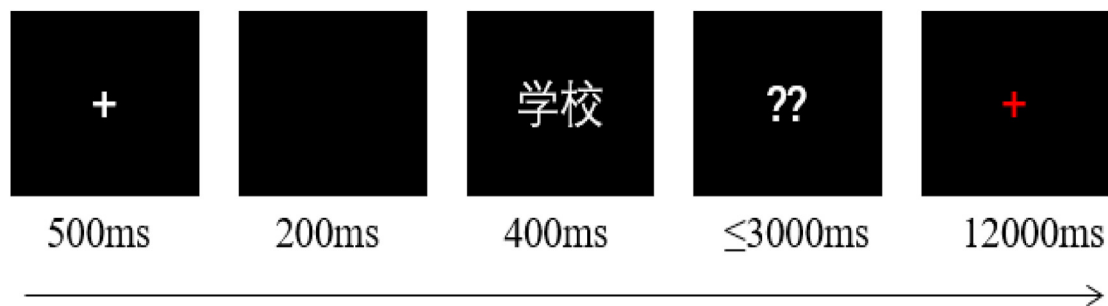
2.4. Concurrent EEG and fNIRS recordings

Both EEG and fNIRS signals were recorded simultaneously while participants were performing the lexical decision task, wearing a fused EEG-fNIRS data acquisition cap (EasyCap, Herrsching, Germany) with reference to the international 10–20 system. EEG data were recorded with 32 Ag/AgCl active electrodes (Brain Products, Munich, Germany) attached to the EEG cap (sampling rate: 500 Hz, bandpass: .03–70 Hz, reference: left mastoid-TP9). Six EEG electrodes were re-located to their neighboring channels due to the pre-emption of fNIRS probes (Fig. 2B). Impedance of each channel was maintained below 25 k Ω before concurrent data acquisition.

⁴ The chance of a syllable/character appearing at a specific position (head or end) in novel Chinese compound words could somehow relate to its word-likeness and acceptability (Ip et al., 2019). The differing position frequencies between real words/pseudowords and nonwords therefore confirms the material validity.

Table 2 – Lexical characteristics of real words, pseudowords, and nonwords.

	Real words		Nonwords		Pseudowords	
	Mean	SD	Mean	SD	Mean	SD
Morphological legality	/	/	2.13	2.05	20.27	2.15
Semantic interpretability	/	/	.08	.07	.74	.14
Stroke number	15.91	3.71	15.13	3.7	15.78	4.23
Word frequency ⁵	105	199	/	/	/	/
Position frequency (head)	.58	.2	.36	.24	.59	.23
Position frequency (end)	.58	.18	.31	.22	.61	.18
Character frequency (head)	581	795	1743	7208	1094	1530
Character frequency (end)	924	1230	876	8560	1358	1622

**Fig. 1 – Experimental procedure of the visual lexical decision task. A slow event-related design was used. “学校”/xue2 xiao4/ denotes “school”.**

Continuous fNIRS data were collected by NIRScout system (NIRx Medizintechnik GmbH, Berlin, Germany) with 8 LED sources and 8 detectors. The optodes (sources and detectors) were placed along the frontal and temporal areas of the left hemisphere (Zhang, 2019; Zhang et al., 2016). The light attenuation was measured at the wavelengths of 760 nm and 850 nm with a sampling rate of 7.81 Hz. The setup yielded 22 measurement channels (Fig. 2B, C, and 2D) with an inter-optode distance of 30 mm.

In addition, the Montreal Neurological Institute (MNI) coordinates of each fNIRS channel were quantified by the use of ICBM-152 head model (ICBM 2009a Nonlinear Symmetric Atlas) and the NIRSite 2.0 toolbox (NIRx Medizintechnik GmbH, Berlin, Germany), which was based on the international 10–20 system for EEG recording (Chatrion, Lettich, & Nelson, 1985; Pfeifer, Scholkmann, & Labruyère, 2018). The coordinates were then imported into the NIRS-SPM software toolbox (Ye, Tak, Jang, Jung, & Jang, 2009) for spatial registration. The spatial configurations (MNI coordinates, BA, anatomical label, and percentage of overlap) of associated 22 channels were provided in Table 3.

2.5. EEG and fNIRS data analysis

The raw EEG data were processed offline using EEGLAB v2021.0 with a re-reference to the mean voltage of the left and right mastoids (TP9, TP10) and a band-pass filter (butterworth filter; filter order: 4) of .01–30 Hz (Chung et al., 2010; Wu et al., 2020). Bad channels were interpolated by using a spherical method. Segmentations from 200 msec pre-stimulus to

800 msec after word onset were carried out, where the measurements of 200 msec pre-stimuli served as the baseline recordings. Independent component analysis (ICA) decomposition was applied by using a “picard” algorithm in EEGLAB. Reoccurring eye artifacts (e.g., eye blinks) and line noise were eliminated by visual inspection. On average, 2.3 (95% CI: 1.57 to 3.03) components were removed across participants. Epochs contaminated with artifacts exceeding $\pm 100 \mu\text{V}$ were rejected for further analysis.

The fNIRS data were processed with nirsLAB (v2019.04, Xu et al., 2019; Pfeifer et al., 2018). The raw data were digitally filtered in the band-pass of .01–.2 Hz to remove drift and respiratory noise with the time period of 2 sec prior to stimulus onset serving as the baseline. Discontinuities and spike artifacts were removed by the built-in algorithms in nirsLAB (std threshold set to 5). After pre-processing, the changes in oxygenated hemoglobin (HbO), deoxygenated hemoglobin (HbR), and total hemoglobin (HbT) responses were then calculated by using the modified Beer–Lambert law equation (Baker et al., 2014; Cope & Delpy, 1988).

As the HbO measure is believed to be a more sensitive indicator of brain activation (e.g., Couto, Wang, & Yuan, 2021; Fu et al., 2014; Hu et al., 2018; Lin et al., 2018), only HbO signals were further analyzed for the present work. For extracting the parameters of brain activity during each of the lexical conditions, HbO time series were modeled using statistical parametric modeling (nirsLAB, SPM Level 1 module) and fitting a canonical hemodynamic response function (HRF, parameters: 6, 16, 1, 1, 6, 0, 32) for estimation of the GLM (general linear model) coefficients, or beta weights. These inclusion/exclusion criteria were established prior to data analysis.

⁵ Frequency: occurrence per million.

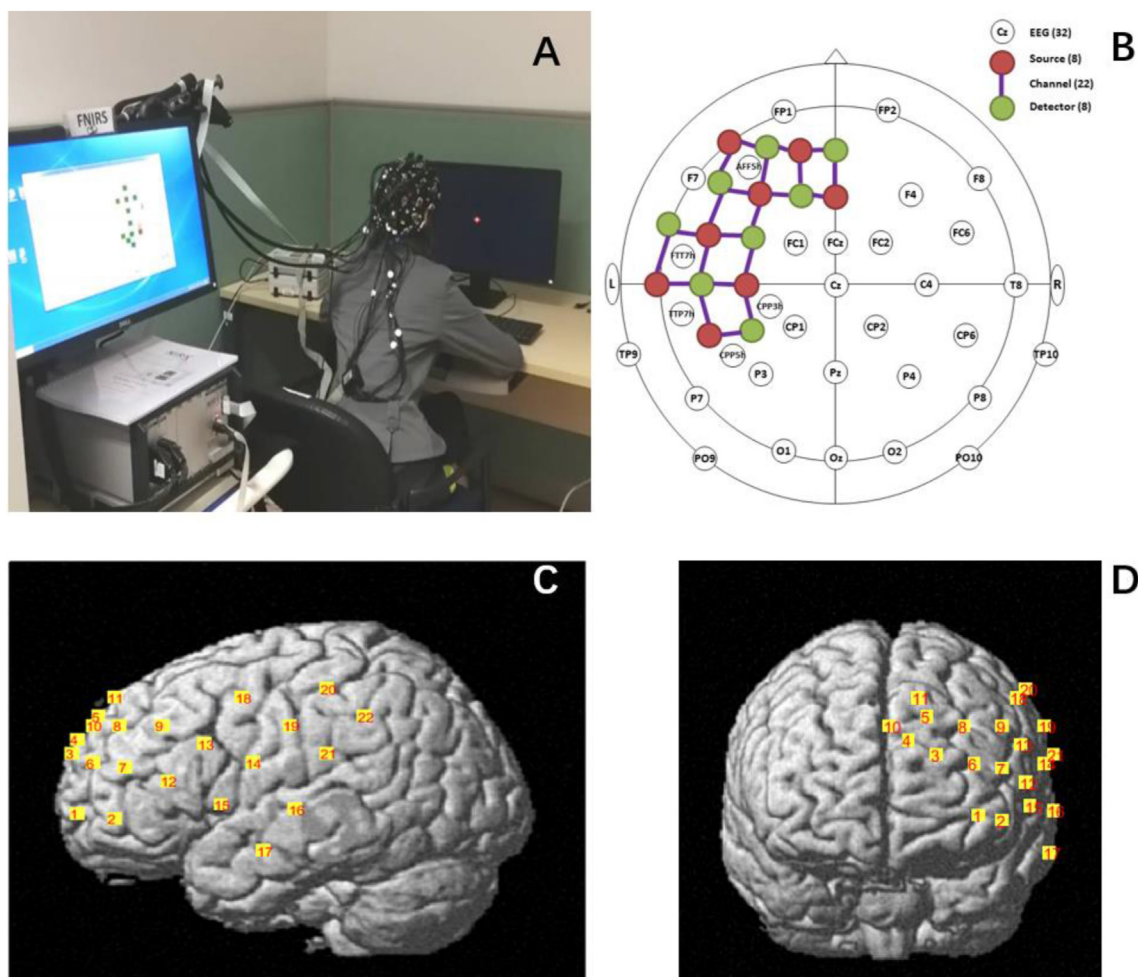


Fig. 2 – EEG-fNIRS setup and channel layout. (A) Schematic of the experimental setup. (B) The configurations of EEG electrodes (white circle), fNIRS sources (red), detectors (green), and channels (purple) along the fused fNIRS-EEG cap. (C) The layout of fNIRS channels in the left view. (D) The layout of the fNIRS channels in the frontal view.

3. Results

3.1. Behavioral results

Behavioral data from two participants was not recorded by experimenter's mistake, leaving data of 28 participants for analysis. First, responses which were incorrect or exceeded ± 3 standard deviations (SD) of the mean reaction time (RT) were treated as outliers and thus excluded before formal analysis. The accuracy rate (ACC) and RT data were then respectively submitted to linear mixed-effect model by lme4 package (Bates, Mächler, Bolker, & Walker, 2014) in RStudio. Lexical condition (three levels: real word, pseudoword, and nonword) was treated as a fixed factor, while participant and word substructure⁶ were set as random factors. ANOVA function from lmerTest package (Kuznetsova, Brockhoff, & Christensen, 2015) was used to examine the main effect of the fixed

factor and multiple comparisons were then performed with pooled t-tests by the emmeans function from the emmeans package. Results revealed a significant main effect of lexical condition for RT data [$F = 322.48, p < .001$]. Pairwise comparisons showed that RT of real words (675.49 ± 5.38 msec) and nonwords (720.73 ± 4.87 msec) was significantly shorter than those of pseudowords (883.63 ± 8.38 msec) ($ps < .05$), while there was no significant difference between real words and nonwords ($p = .215$).

In addition, ACC results also illustrated a reliable main effect of lexical condition, $F = 140.99, p < .001$. It was found that the accurate responses to real words ($95.92\% \pm .57\%$) and nonwords ($98.79\% \pm .31\%$) were significantly higher than that to pseudowords ($75.61\% \pm 1.25\%$), and nonwords were more accurately recognized than real words ($ps < .01$). RT and ACC results were visualized in Fig. 3.

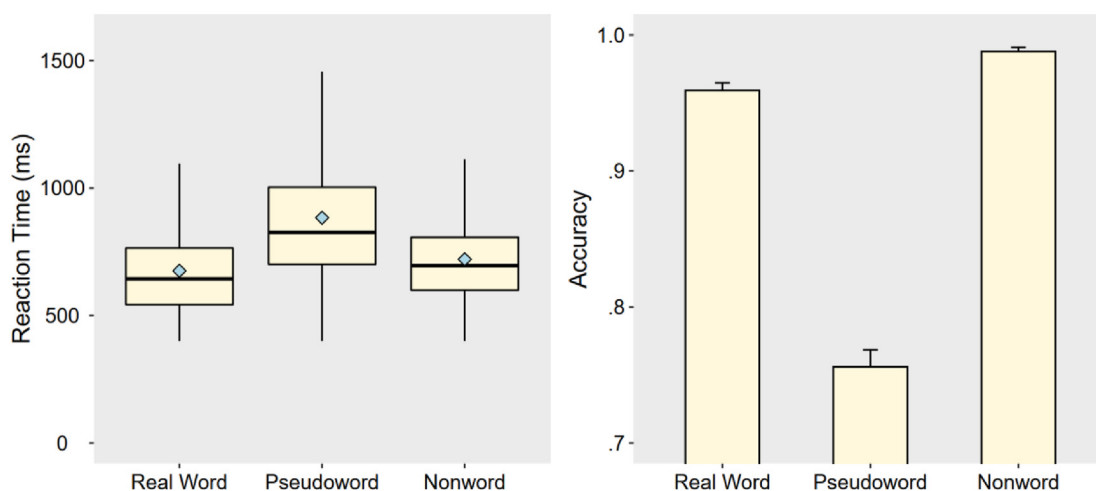
3.2. ERP results

EEG data from five participants were discarded before formal analysis (one with incorrect channel location, one with incorrect trigger information, and three with extensive artifacts),

⁶ “Subordinate, coordinate, verb-object, verb-resultative, subject-predicate” for real words/pseudowords and “none” for nonwords.

Table 3 – The 3D MNI coordinates and associated brain regions of the 22 fNIRS channels.

Channel number	MNI			BA	Anatomical label	Percentage of overlap
	x	y	z			
1	−37.7	63.3	−.7	10	Frontopolar area	1.0
2	−48.0	51.0	−3.0	10	Frontopolar area	.5
				47	Inferior prefrontal gyrus	.4
				46	Dorsolateral prefrontal cortex	.1
3	−19.3	65.3	25.7	10	Frontopolar area	1.0
4	−8.0	64.7	32.0	10	Frontopolar area	.7
5	−15.3	55.3	41.3	9	Dorsolateral prefrontal cortex	.8
6	−36.7	58.0	21.7	10	Frontopolar area	1.0
7	−47.7	45.3	19.7	46	Dorsolateral prefrontal cortex	.8
				10	Frontopolar area	.2
8	−32.7	47.7	37.7	9	Dorsolateral prefrontal cortex	.9
9	−47.0	32.3	37.3	9	Dorsolateral prefrontal cortex	.6
				46	Dorsolateral prefrontal cortex	.3
10	−.3	57.7	37.7	9	Dorsolateral prefrontal cortex	.8
11	−11.0	49.7	49.0	8	Includes Frontal eye fields	.8
12	−57.0	29.3	13.3	45	pars triangularis Broca's area	.7
				46	Dorsolateral prefrontal cortex	.3
13	−56.7	15.7	30.3	9	Dorsolateral prefrontal cortex	.8
14	−65.7	−1.0	21.0	6	Pre-Motor and Supplementary Motor Cortex	.6
15	−60.3	10.3	3.7	22	Superior Temporal Gyrus	.5
16	−69.7	−17.7	2.7	22	Superior Temporal Gyrus	.4
				42	Primary and Auditory Association Cortex	.3
				21	Middle Temporal gyrus	.3
17	−68.0	−6.7	−16.3	21	Middle Temporal gyrus	1.0
18	−54.3	1.3	49.3	6	Pre-Motor and Supplementary Motor Cortex	.9
19	−65.0	−15.3	38.3	6	Pre-Motor and Supplementary Motor Cortex	.5
20	−57.3	−29.3	53.7	2	Primary Somatosensory Cortex	.4
				40	Supramarginal gyrus part of Wernicke's area	.4
21	−69.0	−30.7	25.7	40	Supramarginal gyrus part of Wernicke's area	.7
22	−64.0	−44.3	42.3	40	Supramarginal gyrus part of Wernicke's area	1.0

**Fig. 3 – RT (ms) and ACC for each of the three lexical conditions.**

thus leaving 25 participants.⁷ Based on previous studies, three ERP components were focused on to examine the time course of Chinese morphological encoding and semantic analysis.

⁷ Based on the Reviewer's suggestion, we re-ran the EEG data of 23 participants after removing the two participants whose behavioral data were missing. Likewise, we re-analyzed the fNIRS data of remaining 28 participants. The ERP/activation patterns and statistical analysis results remained unchanged in general.

Specifically, P2a effect (150–180 msec) was investigated in the frontal sites (Gu et al., 2012). N400 (300–450 msec) and LAN components (450–570 msec) were examined in fronto-central and centro-parietal electrodes, whose time windows and regions of interest (ROIs) were suggested by the previous study (Bölte et al., 2009). Scalp topographies and brainwaves from representative electrodes were visualized in Fig. 4.

P2a. A two-way repeated measures ANOVA with Geisser-Greenhouse correction (Greenhouse & Geisser, 1959) was

performed on the frontal P2a (150–180 msec, Gu et al., 2012) amplitudes, with lexical condition and hemisphere (left: AFF5h, FC1, vs right: F4, FC2) as factors. Neither significant main effects of lexical condition [$F(2,48) = 1.057, p = .354$, partial $\eta^2 = .042$]/laterality [$F(1,24) = .02, p = .889$, partial $\eta^2 = .001$], nor reliable interaction [$F(2,48) = 1.273, p = .289$, partial $\eta^2 = .05$] was detected.

N400. According to the topographies of pair-wise difference waves (Fig. 4B), there was a N400-like effect in the fronto-central electrode sites, especially for nonword versus real word contrast. In addition, there was a LAN component in the time window of 450–570 msec, which was pronounced for morphological effect (pseudoword vs real word). We therefore analyzed morphological and semantic effects in the time windows of N400 and LAN, respectively.

A three-way repeated-measures ANOVA was performed on N400 (300–450 msec) amplitudes, with lexical condition, laterality (left: FC1, FTT7h, CCP3h, CP1; midline: FCz, Pz; right: FC2, FC6, CP2, CP6), and region (fronto-central: FC1, FTT7h, FCz, FC2, FC6; centro-parietal: CCP3h, CP1, Pz, CP2, CP6) as variables. The main effect of lexical condition was significant, $F(2,48) = 11.490, p < .001$, partial $\eta^2 = .324$. Further comparisons revealed that the nonword case showed larger negativity ($-1.49 \pm .72 \mu\text{V}$) as compared to the real-word case ($.55 \pm .76 \mu\text{V}$) and pseudowords ($-.25 \pm .81 \mu\text{V}$), although no obvious difference was identified for real word versus pseudoword contrast (comparison results detailed in Table 4). Meanwhile, there was a significant region effect, $F(1,24) = 13.814, p < .01$, partial $\eta^2 = .365$. Greater negativities were

identified in the fronto-central region than in the centro-parietal area ($-.94$ vs $.15 \mu\text{V}, p < .01$). No significant main effect was detected for the laterality, nor any interaction effect.

LAN. Following N400, there was a negative-going component manifested primarily at the left anterior sites (Fig. 4A & 4C). We interpreted this pattern as a LAN effect, which might be linked to the process of structural problem caused by morphological parsing (Bölte et al., 2009). An identical three-way repeated-measures ANOVA revealed a significant main effect of lexical condition, $F(2,48) = 5.807, p < .01$, partial $\eta^2 = .195$. Additional analyses demonstrated that the pseudoword case induced a more negative-going component than real-word case ($.712$ vs $3.027 \mu\text{V}, p < .001$), and the nonword case elicited a larger LAN than the real-word condition (1.461 vs $3.027 \mu\text{V}, p < .05$), whereas no statistical difference was revealed between the pseudowords and nonwords ($p = .36$). Meanwhile, there was a significant interaction effect between lexical condition and laterality, $F(4,96) = 6.229, p < .001$, partial $\eta^2 = .206$. Following-up analyses revealed that pseudowords elicited greater LAN than real words at all sites, while nonwords showed greater LAN only at left and midline electrodes relative to real words ($ps < .01$). No significant main effect for the region and any other interaction was found.

3.3. fNIRS results

Standardized beta values (Z-scores) were submitted to an all-encompassing linear mixed-effect model with participant and fNIRS channel as the random factors and lexical condition as

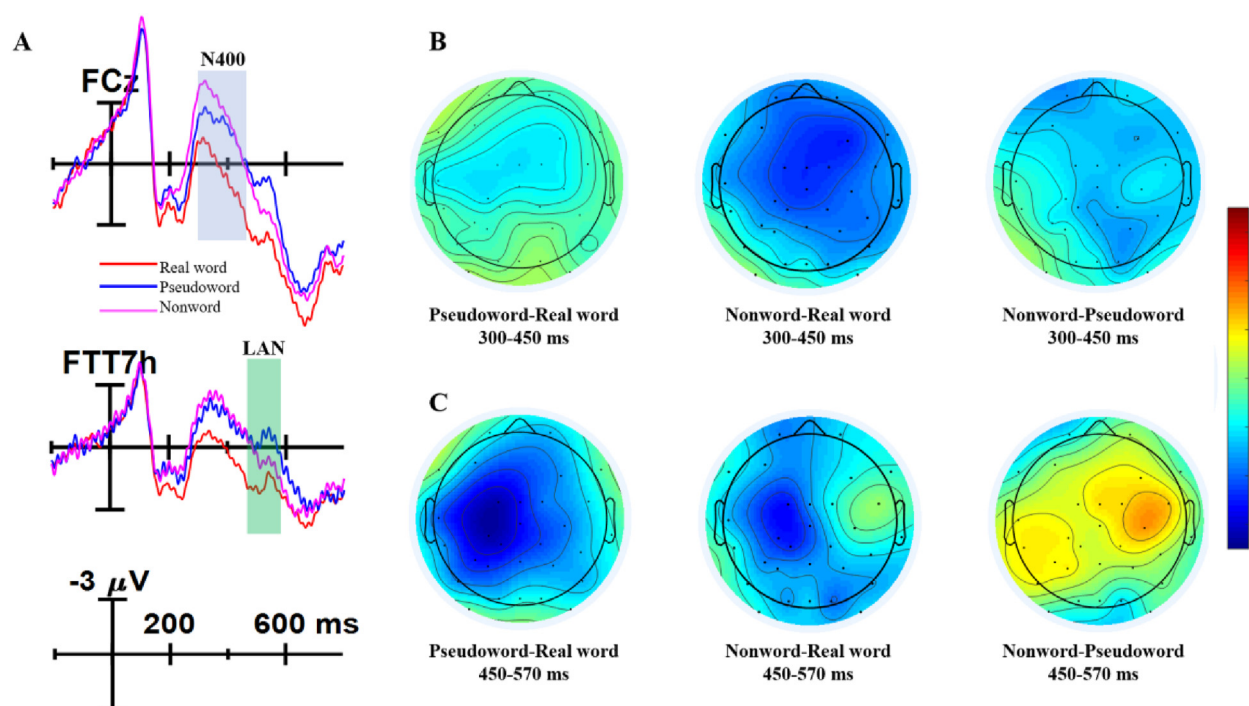


Fig. 4 – Grand-averaged ERPs on representative electrodes and voltage difference maps showing N400 and LAN effects. N400 exhibits its significance between the three conditions along the fronto-central sites [FCz of sub-figure A and topographies of B], especially in nonword versus real word comparison. Meanwhile, anterior negativity is more left lateralized [FTT7h of sub-figure A and topographies of C], especially for pseudoword versus real word comparison.

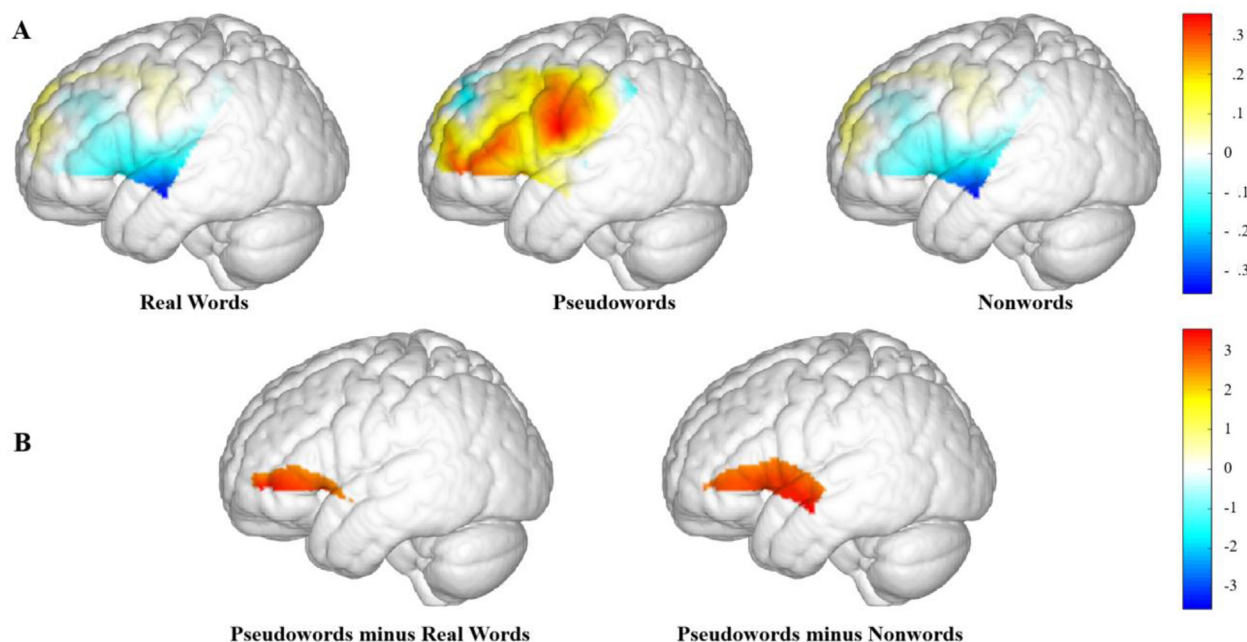


Fig. 5 – Brain activation patterns associated with three lexical conditions and pairwise comparisons. (A) Brain activation associated with three lexical conditions. Colorbar denotes the standardized beta values. (B) Brain maps of t values of standardized beta value contrast between the three lexical conditions. T values ($p < .01$ for visualization purpose) are displayed according to the colorbar. Morphological encoding (pseudowords vs real words) employs the left frontopolar area and the IFG, while semantic processing (pseudowords vs nonwords) engages a broader network including the left frontal and temporal cortex (STG and MTG). There is no significant difference in the real-word versus nonword contrast.

Chinese complex word recognition. This finding from Chinese compound words is in line with German and Finnish pseudoword studies (Janssen, Wiese, & Schlesewsky, 2006; Leinonen et al., 2008), which showed that the violations of derivational rules would engage a semantic analysis earlier than structural parsing. As nonwords are novel stimuli of zero frequency, participants might need to firstly decompose them into familiar constitute characters and then try to generate the possible semantic relationship. Therefore, the brain activation difference between nonwords and real words/pseudowords at 300–450 msec might suggest the meaning retrieval at sub-lexical level, in favor of a morphological decomposition account (Feldman, Frost, & Pnini, 1995; Huang et al., 2011a,b).

After the early N400 semantic modulation, morphological legality effect was then detected by the neural activation difference at 450–570 msec. The present results showed that pseudowords were able to induce significantly larger and later negativities than real words, which were pronounced in anterior sites. Even the current statistical analyses did not reveal a reliable lateralization in the left hemisphere, the topographies clearly showed a leftward distribution of this negativity. We therefore interpreted this component as a

LAN effect indexing a rather pure morphological encoding, as morphological sensitivity primarily constitutes the difference between pseudowords and real words. This result replicated findings from the German pseudoword study (Bölte et al., 2009), where semantically interpretable yet structurally non-existing pseudowords elicited enhanced LAN than existing adjectives embedded in sentences. As such, LAN might be more sensitive to the morphological status in complex Chinese word recognition, which somehow overlaps the function of morphological P600 (Gu and Yang, 2010). Although pseudowords follow the morphological structure rules, participants might need to consume extra cognitive efforts to scrutinize the word's structural organization when they encounter difficulties in a conventional semantic analysis. For example, for the pseudo compound word “微笑”, participants might firstly need to access the meaning of constitute morpheme respectively (i.e., “mild” plus “crying”), which is interpretable semantically. Yet, it is hard for them to map the word's structure to any existing entry in mental lexicon when trying to decide its legality. Therefore, this late ERP component indicates that there exists a conscious and controlled process working well

Table 5 – fNIRS channels showing significant comparison results after FDR correction.

Channel	Comparison	t	p (uncorrected)	p (FDR corrected)
2	Pseudowords minus Real Words	3.523	.001	.004
2	Pseudowords minus Nonwords	2.716	.011	.017
15	Pseudowords minus Nonwords	2.94	.023	.006
17	Pseudowords minus Nonwords	3.385	.002	.006

with morphological constraints (Allen et al., 2003; Newman et al., 2007; Gu and Yang, 2010).

Interestingly, the current study found a biphasic pattern of semantic N400 and structural LAN in single word comprehension, while evidence from alphabetic languages only identified a singular pattern of LAN in pseudoword decoding (e.g., Bölte et al., 2009). This discrepancy could be attributed to linguistic topography and stimulus type. In particular, the study on German words employed derivational morphology, where structural parsing might outweigh semantic analysis due to the extensive online computation. By contrast, each character represents a morpheme in Chinese compound words. It might give rise to a semantic analysis at the morphemic level before the morphological parsing.

It is worth noting that the temporal neural activation difference between nonwords and real words was persistent across both earlier and later time windows (from 300–450 msec to 450–570 msec). This pattern suggested that semantic analysis at morphemic level occurred earlier till the content of stimuli were cracked. In particular, LAN effect for pseudoword recognition indicated that these constituents are further processed holistically after decomposition and re-composition. These findings collectively shed light upon the relative independence of morphological constraint, which might encode a controlled process of neural resources.

Alternatively, one might argue that the observed ERP component related to morphological constraint might be confounded with frequency and semantic contaminations, as there existed differences between real words and pseudowords regarding these two factors. However, word frequency and semantic analysis often took place in earlier time windows like N400 (see review by Lau, Phillips, & Poeppel, 2008), while LAN has been widely recognized as the indicator of structural problems, such as morpho-syntactic error and phrase-structure building (Bölte et al., 2009; Hahne & Friederici, 2002; Linares, Rodriguez-Fornells, & Clahsen, 2006). We therefore postulated that the late negativity identified in 450–570 msec is largely due to structural sensitivity and morphological encoding in single compound word reading.

Further, it is noted from previous studies that ERP components P2a (Chung et al., 2010; Gu et al., 2012) might be associated with the processing of Chinese morphological structure information. Nevertheless, this is not the case for the present study. Specifically, the previous work adopted a priming paradigm to examine how morphological structure modulated lexical access, in which the stimulus onset asynchronies (SOA) was set at 57 msec and 200 msec, respectively. As such, the detected P2a effect in previous studies might reflect the special demands from structural priming rather than word reading in isolations. This merits further investigations in the future.

4.3. The spatial brain activation patterns for morphological constraints

Relative to EEG signals, fNIRS is able to better map the spatial brain activation patterns associated with neural activities, by tracking the hemodynamic changes in light of the neuro-vascular coupling mechanism. In this study, channel-wise

analyses demonstrated that the left prefrontal cortex is primarily involved in Chinese morphological constraint processing. Importantly, we discovered that the left prefrontal network (BA 10/47), including the IFG, is sensitive to morphological regularity in pseudowords versus real words contrast, which overlaps the localizations of semantic analysis. Yet, the spatial brain activation difference between the semantic regulars and irregulars (pseudowords/nonwords vs nonwords) employed significantly broader networks, extending from the left prefrontal cortex to the MTG (BA 21) and the STG (BA 22). The present findings therefore shed light upon a differentiation between the neural engagements of morphological parsing and semantic analysis (i.e., the left IFG and the broader fronto-temporal network, respectively).

Especially, the role of the ventral aspect of the left IFG (BA47) in Chinese morphological processing was manifested (as shown in Fig. 5). More importantly, previous reports demonstrated that young English-speaking children showed significant brain activation in the left IFG during an auditory morphological awareness task, which was comparable to the patterns obtained from young Chinese children (Arredondo et al., 2015). Similar results were reported in studies with Chinese-speaking adults performing auditory morphological judgment task (Zou et al., 2016). Their results confirmed that the left IFG is a core area for morphological processing across various languages. Therefore, the present work further revealed that the left IFG might be prominent in single Chinese words processing involved in morphological constraints regardless of the language modalities (visual or auditory).

Besides the left frontal activation, previous studies also reported the involvement of the left temporal cortex in morphological processing (e.g., Hsu et al., 2019; Ip et al., 2019). Yet, the present study did not detect a significant brain activation difference in reading Chinese words between various morphological constraints in the left temporal region. This could be attributed to the relatively limited spatial resolution and channel numbers of the fNIRS used in the current study. Future studies could further examine this region by using broader cortex coverage of fNIRS or functional magnetic resonance imaging (fMRI) techniques.

In summary, EEG recordings showed that morphological processing of morpho-syllabic compound words are carried out at the later stage of lexical processing, while concurrent fNIRS data demonstrated that the left prefrontal cortex (especially the IFG) plays an important role in this process. From a technological perspective, fused EEG-fNIRS constitutes a viable tool inspecting *when*, *where*, and *how* morphological processing was encoded in cerebral cortex during language reading.

Conflict of Interest

No potential conflict of interest was reported by the authors.

Data availability statement

Study materials and data are available online: <https://osf.io/2s3jx/>

CRediT author statement

Fei Gao: Conceptualization, Methodology, Formal analysis, Investigation, Writing - Original Draft, Writing - Review & Editing, Visualization. Ruien Wang: Methodology, Software, Investigation, Data Curation. Paulo Armada-da-Silva: Validation, Data Curation, Writing - Review & Editing. Meng-Yun Wang: Methodology, Software, Formal analysis. Hai Lu: Validation, Writing - Review & Editing. Chantat Leong: Investigation, Writing - Review & Editing. Zhen Yuan: Conceptualization, Resources, Writing - Review & Editing, Supervision, Project administration, Funding acquisition.

Open practices

The study in this article earned Open Data and Open Materials badges for transparent practices. Materials and data for the study are available at <https://osf.io/2s3jx/>.

Acknowledgment

This work was supported by the University of Macau (MYRG 2020-00067-FHS, MYRG2019-00082-FHS and MYRG2018-00081-FHS), the Macao Science and Technology Development Fund (FDCT 0020/2019/AMJ and FDCT 0011/2018/A1), and Higher Education Fund of Macao SAR Government (CP-UMAC-2020-01). We would also like to thank Mr. Yuwen He, Mr. Lin Hua, Ms. Jianhua Li, Mr. Jianhang Zhou, and Dr. Juliet Chen for their assistance in data analysis.

REFERENCES

- Allen, M., Badecker, W., & Osterhout, L. (2003). Morphological analysis in sentence processing: An ERP study. *Language and Cognitive Processes, 18*(4), 405–430.
- Arredondo, M. M., Ip, K. I., Shih Ju Hsu, L., Tardif, T., & Kovelman, I. (2015). Brain bases of morphological processing in young children. *Human Brain Mapping, 36*(8), 2890–2900.
- Baker, W. B., Parthasarathy, A. B., Busch, D. R., Mesquita, R. C., Greenberg, J. H., & Yodh, A. G. (2014). Modified Beer-Lambert law for blood flow. *Biomedical Optics Express, 5*(11), 4053–4075.
- Bates, D., Mächler, M., Bolker, B., & Walker, S. (2014). *Fitting linear mixed-effects models using lme4*. arXiv preprint arXiv:1406.5823.
- Bick, A. S., Frost, R., & Goelman, G. (2010). Imaging implicit morphological processing: Evidence from Hebrew. *Journal of Cognitive Neuroscience, 22*(9), 1955–1969.
- Bölte, J., Jansma, B. M., Zilverstand, A., & Zwitserlood, P. (2009). Derivational morphology approached with event-related potentials. *The Mental Lexicon, 4*(3), 336–353.
- Booth, J. R., Lu, D., Burman, D. D., Chou, T. L., Jin, Z., Peng, D. L., ... Liu, L. (2006). Specialization of phonological and semantic processing in Chinese word reading. *Brain Research, 1071*(1), 197–207.
- Carrasco-Ortiz, H., & Frenck-Mestre, C. (2014). Phonological and orthographic cues enhance the processing of inflectional morphology. ERP evidence from L1 and L2 French. *Frontiers in Psychology, 5*, 888.
- Chatrian, G. E., Lettich, E., & Nelson, P. L. (1985). Ten percent electrode system for topographic studies of spontaneous and evoked EEG activities. *American Journal of EEG technology, 25*(2), 83–92.
- Chee, M. W., O'Craven, K. M., Bergida, R., Rosen, B. R., & Savoy, R. L. (1999). Auditory and visual word processing studied with fMRI. *Human Brain Mapping, 7*(1), 15–28.
- Chung, K. K., Tong, X., Liu, P. D., McBride-Chang, C., & Meng, X. (2010). The processing of morphological structure information in Chinese coordinative compounds: An event-related potential study. *Brain Research, 1352*, 157–166. <https://doi.org/10.1016/j.brainres.2010.06.069>
- Cope, M., & Delpy, D. T. (1988). System for long-term measurement of cerebral blood and tissue oxygenation on newborn infants by near infra-red transillumination. *Medical & Biological Engineering & Computing, 26*(3), 289–294.
- Couto, T. A., Wang, M. Y., & Yuan, Z. (2021). Optical neuroimaging of executive function impairments in food addiction. *Journal of Innovative Optical Health Sciences, Article 2250005*.
- DeFrancis, J. (1989). *Visible speech: The diverse oneness of writing systems*. University of Hawaii Press.
- Feldman, L. B., Frost, R., & Pnini, T. (1995). Decomposing words into their constituent morphemes: Evidence from English and Hebrew. *Journal of Experimental Psychology: Learning, Memory, and Cognition, 21*(4), 947.
- Fu, G., Mondloch, C. J., Ding, X. P., Short, L. A., Sun, L., & Lee, K. (2014). The neural correlates of the face attractiveness aftereffect: A functional near-infrared spectroscopy (fNIRS) study. *Neuroimage, 85*, 363–371.
- Gao, F., Wang, J., Zhao, C. G., & Yuan, Z. (2021). Word or morpheme? Investigating the representation units of L1 and L2 Chinese compound words in mental lexicon using a repetition priming paradigm. *International Journal of Bilingual Education and Bilingualism, 1–15*.
- Gu, J., & Yang, Y. (2010). A neuro-electrophysiological study on productivity of Chinese compounding [in Chinese]. *Applied Linguistics (in China), 3*, 98–107.
- Gu, J., Yu, L., & Ma, P. (2012). P2a reflects morphology structural processes in brain: Evidence from ERPs [in Chinese]. *Journal of Southwest University (Natural Science Edition), 34*(2), 137–144.
- Hahne, A., & Friederici, A. D. (2002). Differential task effects on semantic and syntactic processes as revealed by ERPs. *Cognitive Brain Research, 13*(3), 339–356.
- Hsu, C. H., Pylkkänen, L., & Lee, C. Y. (2019). Effects of morphological complexity in left temporal cortex: An MEG study of reading Chinese disyllabic words. *Journal of Neurolinguistics, 49*, 168–177.
- Huang, C. Y., Lee, C. Y., Huang, H. W., & Chou, C. J. (2011a). Number of sense effects of Chinese disyllabic compounds in the two hemispheres. *Brain and Language, 119*(2), 99–109. <https://doi.org/10.1016/j.bandl.2011.04.005>
- Huang, H. W., Lee, C. Y., Tsai, J. L., & Tzeng, O. J. (2011b). Sublexical ambiguity effect in reading Chinese disyllabic compounds. *Brain and Language, 117*(2), 77–87. <https://doi.org/10.1016/j.bandl.2011.01.003>
- Huang, B. R., & Liao, X. D. (2011). *Xiandai Hanyu [in Chinese]*. Beijing: Higher Education Press.
- Hu, Z., Zhang, J., Couto, T. A., Xu, S., Luan, P., & Yuan, Z. (2018). Optical mapping of brain activation and connectivity in occipitotemporal cortex during Chinese character recognition. *Brain Topography, 31*(6), 1014–1028.
- Ip, K. I., Marks, R. A., Hsu, L. S., Desai, N., Kuan, J. L., Tardif, T., et al. (2019). Morphological processing in Chinese engages left temporal regions. *Brain and Language, 199*, Article 104696. <https://doi.org/10.1016/j.bandl.2019.104696>
- Janssen, U., Wiese, R., & Schlesewsky, M. (2006). Electrophysiological responses to violations of morphosyntactic and prosodic features in derived German nouns. *Journal of Neurolinguistics, 19*(6), 466–482.

- Jin, G., Xiao, H., Fu, L., & Zhang, Y. (2005). The construction and deep processing of Modern Chinese Corpus [in Chinese]. *Applied Linguistics (China)*, 2, 111–120.
- Kuznetsova, A., Brockhoff, P. B., & Christensen, R. H. B. (2015). Package 'lmerTest'. *R package version*, 2, 734.
- Lau, E. F., Phillips, C., & Poeppel, D. (2008). A cortical network for semantics:(de) constructing the N400. *Nature reviews neuroscience*, 9(12), 920–933.
- Leinonen, A., Brattico, P., Järvenpää, M., & Krause, C. M. (2008). Event-related potential (ERP) responses to violations of inflectional and derivational rules of Finnish. *Brain research*, 1218, 181–193.
- Leminen, A., Smolka, E., Dunabeitia, J. A., & Pliatsikas, C. (2019). Morphological processing in the brain: The good (inflection), the bad (derivation) and the ugly (compounding). *Cortex; a Journal Devoted To the Study of the Nervous System and Behavior*, 116, 4–44.
- Leong, C. K., Cheng, P. W., & Tan, L. H. (2005). The role of sensitivity to rhymes, phonemes and tones in reading English and Chinese pseudowords. *Reading and Writing*, 18(1), 1–26.
- Liao, W. (2014). Morphology. In C. T. J. Huang, Y. H. A. Li, A. Simpson, & J. Wiley (Eds.), *The handbook of Chinese linguistics* (pp. 1–25). Hoboken, NJ: Wiley-Blackwell.
- Linares, R. E., Rodriguez-Fornells, A., & Clahsen, H. (2006). Stem allomorphy in the Spanish mental lexicon: Evidence from behavioral and ERP experiments. *Brain and Language*, 97(1), 110–120.
- Lin, X., Lei, V. L. C., Li, D., Hu, Z., Xiang, Y., & Yuan, Z. (2018). Mapping the small-world properties of brain networks in Chinese to English simultaneous interpreting by using functional near-infrared spectroscopy. *Journal of Innovative Optical Health Sciences*, 11(3), Article 1840001.
- Liu, L., Deng, X., Peng, D., Cao, F., Ding, G., Jin, Z., ... Deng, Y. (2009). Modality-and task-specific brain regions involved in Chinese lexical processing. *Journal of Cognitive Neuroscience*, 21(8), 1473–1487.
- Liu, L., Tao, R., Wang, W., You, W., Peng, D., & Booth, J. R. (2013). Chinese dyslexics show neural differences in morphological processing. *Developmental Cognitive Neuroscience*, 6, 40–50.
- Longtin, C. M., & Meunier, F. (2005). Morphological decomposition in early visual word processing. *Journal of Memory and Language*, 53(1), 26–41.
- Luck, S. J. (2014). *An introduction to the event-related potential technique*. MIT press.
- McKinnon, R., Allen, M., & Osterhout, L. (2003). Morphological decomposition involving non-productive morphemes: ERP evidence. *Neuroreport*, 14(6), 883–886.
- Meunier, F., & Longtin, C. M. (2007). Morphological decomposition and semantic integration in word processing. *Journal of Memory and Language*, 56(4), 457–471.
- Morris, J., & Holcomb, P. J. (2005). Event-related potentials to violations of inflectional verb morphology in English. *Cognitive Brain Research*, 25(3), 963–981.
- Newman, A. J., Ullman, M. T., Pancheva, R., Waligura, D. L., & Neville, H. J. (2007). An ERP study of regular and irregular English past tense inflection. *Neuroimage*, 34(1), 435–445.
- Noble, W. S. (2009). How does multiple testing correction work? *Nature Biotechnology*, 27(12), 1135–1137.
- Oldfield, R. C. (1971). The assessment and analysis of handedness: The Edinburgh inventory. *Neuropsychologia*, 9(1), 97–113.
- Pan, X., & Jared, D. (2020). Effects of Chinese word structure on object categorization in Chinese–English bilinguals. *Language and Cognition*, 12(3), 468–500.
- Pfeifer, M. D., Scholkmann, F., & Labruyère, R. (2018). Signal processing in functional near-infrared spectroscopy (fNIRS): Methodological differences lead to different statistical results. *Frontiers in Human Neuroscience*, 11, 641.
- Pylkkänen, L., Feintuch, S., Hopkins, E., & Marantz, A. (2004). Neural correlates of the effects of morphological family frequency and family size: An MEG study. *Cognition*, 91, 35–45.
- Pylkkänen, L., & Marantz, A. (2003). Tracking the time course of word recognition with MEG. *Trends in Cognitive Sciences*, 7(5), 187–189.
- Rossi, S., Gugler, M. F., Friederici, A. D., & Hahne, A. (2006). The impact of proficiency on syntactic second-language processing of German and Italian: Evidence from event-related potentials. *Journal of cognitive neuroscience*, 18(12), 2030–2048.
- Schremm, A., Novén, M., Horne, M., & Roll, M. (2019). Brain responses to morphologically complex verbs: An electrophysiological study of Swedish regular and irregular past tense forms. *Journal of Neurolinguistics*, 51, 76–83.
- Su, B. R. (2016). The implicit, diversity and cognitive features of Chinese compounding [in Chinese]. *Academic Research*, 1, 162–165.
- Tseng, H., Lindsay, S., & Davis, C. J. (2020). Semantic interpretability does not influence masked priming effects. *The Quarterly Journal of Experimental Psychology: QJEP*, 73(6), 856–867.
- Wu, J., Chang, J., Qiu, Y., & Joseph, D. (2020). The temporal process of visual word recognition of Chinese compound: Behavioral and ERP evidences based on homographic morphemes. *Acta Psychologica Sinica*, 52(2), 113–127.
- Xu, Y., Graber, H. L., Schmitz, C. H., & Barbour, R. L. (2019). *nirsLAB: A problem-solving environment for fNIRS neuroimaging data analysis*.
- Ye, J. C., Tak, S., Jang, K. E., Jung, J., & Jang, J. (2009). NIRS-SPM: Statistical parametric mapping for near-infrared spectroscopy. *Neuroimage*, 44(2), 428–447.
- Zhang, Y. (2019). *The research of abstract words semantic representation and brain mechanism for Tibetan-Chinese bilinguals [in Chinese]*. Hebei Normal University Dissertation.
- Zhang, P., Zhang, Q., Peng, G., & Bai, X. (2016). The representation of Chinese two-character words in mental lexicon: Evidence from an fNIRS study [in Chinese]. *Journal of Psychological Science*, 39(4), 849–855.
- Zhao, S., Wu, Y., Li, T., & Guo, Q. (2017). Morpho-semantic processing in Chinese word recognition: An ERP study [in Chinese]. *Acta Psychologica Sinica*, 49(3), 296–306.
- Zou, L., Packard, J. L., Xia, Z., Liu, Y., & Shu, H. (2016). Neural correlates of morphological processing: Evidence from Chinese. *Frontiers in Human Neuroscience*, 9, 714.